COBEM 2023 27TH INTERNATIONAL CONGRESS OF MECHANICAL ENGENEERING

ABCM Brazilian Society of Mechanical Sciences and Engineering
27th ABCM International Congress of Mechanical Engineering
December 04-08, 2023, Florianópolis-SC, Brazil

COB-2023-1468
INFLUENCE OF A NON-CONTINUOUS AND UNILATERAL ELASTIC BASE ON THE NONLINEAR VIBRATIONS OF A CYLINDRICAL PANEL

Jordana L. Morais
Frederico M. A. Silva
School of Civil and Environmental Engineering, Federal University of Goiás
University Avenue nº. 1488, 74605-200, Goiás, Goiânia, Brazil
e-mails: jordanalopes@discente.ufg.br, silvafma@ufg.br

Abstract. *Cylindrical panels are structural elements that have applications in many engineering fields as civil, aerospatial, and mechanical engineering, among others. Generally, to prescribe their behavior and stability under dynamic loads, the mathematical model must consider their geometric nonlinearities and contact with an elastic medium. Thus, the objective of this work is to investigate the influence of a non-continuous, unilateral elastic base and an initial geometric imperfection on the nonlinear vibrations of a simply supported cylindrical panel. The cylindrical panel is described by the Donnell's nonlinear shallow shell theory and is discretized using the Galerkin method. To reduce the set of the discretized equations of the dynamical system, a perturbation method is employed to derive a reduced-order model. The non-continuous elastic base model is represented by a Heaviside function, and the unilateral contact is defined using the Signum function. To provide a thorough analysis, the study presents a dynamic analysis of the cylindrical panel through backbone curves, bifurcation diagrams, phase portraits, and resonance curves. These results provide a comprehensive understanding of the impact of the non-continuous, unilateral elastic base and the initial geometric imperfection on the cylindrical panel. A two-degree-of-freedom efficient modal solution is employed to sufficiently describe the nonlinear softening behavior of the cylindrical panel. The numerical results reveal that the non-continuous, unilateral elastic base and the initial geometric imperfection have significant effects on the dynamic stability of the cylindrical panel, showing some Neimark-Sacker bifurcation points in the resonance curves. Moreover, the stable and unstable regions of the resonance curves exhibit important changes when compared with a cylindrical panel featuring a non-continuous, bilateral elastic base. In conclusion, this study provides valuable insights into the effects of non-continuous, unilateral elastic bases and initial geometric imperfections on the nonlinear vibrations of simply supported cylindrical panels.*

Keywords: *cylindrical panel, unilateral elastic base, initial geometric imperfection*

1. INTRODUCTION

Cylindrical panels, also known as open circular cylindrical shells, are structural elements with applications in many fields: engineering civil, aero spatial and mechanical engineering, among others. These structural elements usually are slenderness, so it is necessary to consider their geometric nonlinearities in the mathematical model to describe their behavior and stability under static and dynamic loads. Reviews of the literature about cylindrical panels are found in the works of Amabili e Paidoussis (2003), Alijani e Amabili (2014), Martins et al. (2018) where these papers present several cylindrical panels works under different loadings, strain fields, materials, boundary condition, among so many issues.

In the works of Younesian et al. (2019), Malekjafarian et al. (2021), Lamprea-Pineda et al. (2022) and Zhao et al. (2022) the analyzes are for vibrations in different structural systems, such as beams, plates, cables, membranes, shells and cylindrical panels, supported on an elastic foundation. The first studies on a unilateral foundation can be attributed to Yechiel Weitsman (1971) where the analyzes were obtained for an Euler-Bernoulli beam, subjected to a concentrated mobile load, and supported on a unilateral elastic base reacting only for compression. Since then, many works have investigated the non-linear behavior of structures for different types of stiffness of the foundation or discontinuous elastic base in the domain of the structural system, as the works of Amabili e Dalpiaz (1997), Tj et al. (2006), Silveira et al. (2008), Kim (2015), Bahadori e Najafizadeh (2015), Bhattiprolu, Bajaj e Davies (2016), Yang et al. (2019), Babaei e Eslami (2021), Song et al. (2022), Morais e Silva (2022).

This work aims to analyze the influence of a discontinuous unilateral elastic base in the nonlinear dynamic behavior of a geometrically imperfect cylindrical panel. The cylindrical panel is described by Donnell's nonlinear theory, discretized by the Galerkin method and a reduced order model obtained by a perturbation method. The discontinuous elastic base with unilateral contact is described by a mathematical model that employs the Heaviside and Signum functions.

2. PROBLEM FORMULATION

An imperfect circular cylindrical panel, simply supported and of thin-walled, with radius R, thickness h, axial length a_x, circumferential length a_θ, and open-angle $\Theta[=a_\theta/R]$, is considered, as shown in Figure 1a. Its material is assumed as linear elastic, isotropic and homogenous with Young's modulus E, Poisson's coefficient ν, and density ρ. The displacement fields in the axial, u, circumferential, v, and transversal, w directions are also represented in Figure 1a with their cylindrical coordinates x, θ, and z, respectively. The Donnell's non-linear shallow shell theory is considered, and the nonlinear equation of motion and the compatibility equation of the cylindrical panel are given in terms of the transversal displacement field w and the Airy's stress function f, by:

$$\begin{aligned}\rho h w_{,tt} + 2\eta_1 \rho h \omega_0 w_{,t} + D\left(w_{,xxxx} + \frac{2}{R^2} w_{,\theta\theta xx} + \frac{1}{R^4} w_{x\theta\theta\theta}\right) - f_{,\theta\theta}(w_{,x} + w_{0,x})_{,x} + Rf_{,xx} - f_{,xx}(w_{,\theta} \\ + w_{0,\theta})_{,\theta} - 2f_{x\theta}(w_{,\theta x} + w_{0,\theta x}) + p_k - p(t) = 0 \\ \nabla^4 f = \frac{Eh}{R^4}\left(w_{,x\theta}^2 - w_{,xx} w_{,\theta\theta} + R w_{,xx} + 2 w_{,x\theta} w_{0,x\theta} - w_{,xx} w_{0,\theta\theta} - w_{,\theta\theta} w_{0,xx}\right)\end{aligned} \tag{1}$$

where ω_0 is the fundamental frequency of the perfect cylindrical panel, η_1 is the viscous damping factor, $D[=Eh^3/12(1-\nu^2)]$ is the flexural stiffness. w_0 is an initial geometrical imperfection, $p(t)$ is the time-dependent transversal load, and p_k is the reaction of the discontinuous unilateral elastic base, being described, respectively, by:

$$\begin{aligned} w_0 &= W_0^{imp} h \sin\left(\frac{m\pi x}{a_x}\right) \sin\left(\frac{n\pi\theta}{\Theta}\right) \\ p(t) &= P_L \sin\left(\frac{m\pi x}{a_x}\right) \sin\left(\frac{n\pi\theta}{\Theta}\right) \cos(\omega_L t) \\ p_k &= \left[K_w w + K_P\left(w_{,xx} + \frac{w_{,\theta\theta}}{R^2}\right)\right] H_x H_\theta \frac{(1 - sgn\, w)}{2} \end{aligned} \tag{2}$$

where P_L is the magnitude of transversal load, ω_L is the excitation frequency, and K_w and K_P are the Winkler and Pasternak stiffness parameters, respectively. The discontinuous elastic base is described by the Heaviside function $H_x = H(x-\varepsilon_1) - H(x-\varepsilon_2)$ in the longitudinal direction with the contact region defined by $0 \leq \varepsilon_1 < \varepsilon_2 \leq L$, Figure 1b, while for the circumferential direction, the Heaviside function is $H_\theta = H(\theta-\varepsilon_3) - H(\theta-\varepsilon_4)$ in the contact region with the limits $0 \leq \varepsilon_3 < \varepsilon_4 \leq \Theta$, Figure 1c. The Signum function, *sgn*, controls the unilateral contact of elastic base, i.e., when w presents positive values, the reaction p_k becomes zero. For a discontinuous elastic base with bilateral contact, the term (1-*sgn* w)/2 in Eq. (2) is replaced by 1.

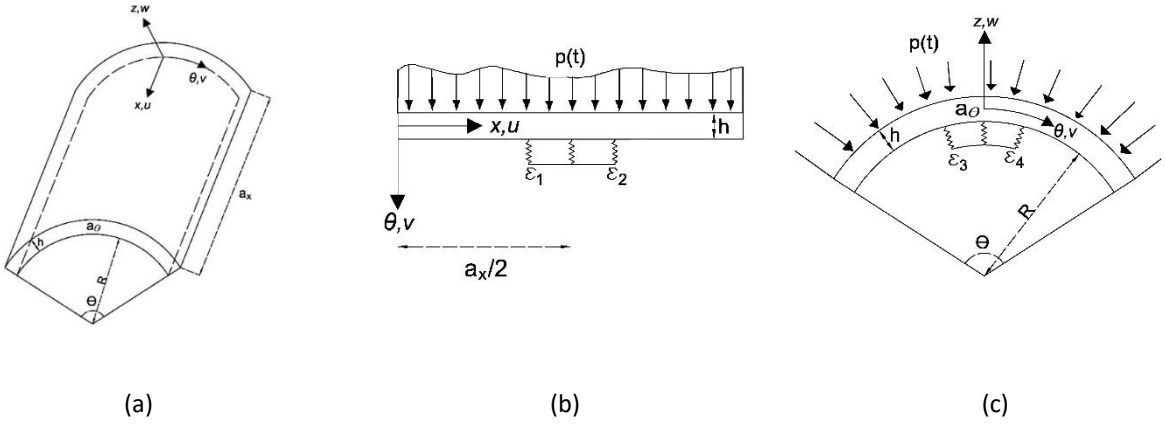

(a) (b) (c)

Figure 1. (a) Geometry, displacement field and coordinate system of the cylindrical panel. (b) Elastic foundation in the longitudinal direction, contact region defined by $0 \leq \varepsilon_1, \varepsilon_2 \leq L$. (c) Elastic foundation in the circumferential direction, contact region defined by $0 \leq \varepsilon_3, \varepsilon_4 \leq \Theta$.

Airy stress function, *f*, is obtained analytically for a particular transversal displacement field *w*. According to Morais and Silva (2019), a consistent transversal displacement field is derived from a perturbation method, for a simply supported cylindrical panel, with the following general modal solution: by:

$$
\begin{aligned}
w = & \sum_{i=1,3,5}\sum_{j=1,3,5} C_{1,_{ij}}(t)\sin\left(\frac{im\pi x}{a_x}\right) sin\left(\frac{jn\pi\theta}{\Theta}\right) \\
& + \sum_{\alpha=0,1,2,3\ldots}\sum_{\beta=0,1,2,3\ldots} C_{2,(2+6\alpha)(2+6\beta)}(t)\left\{\left[\frac{3+6\alpha}{4+12\alpha}\cos\left(\frac{6\alpha m\pi x}{a_x}\right) - \cos\left(\frac{(2+6\alpha)m\pi x}{a_x}\right)\right.\right. \\
& \left.\left. + \frac{1+6\alpha}{4+12\alpha}\cos\left(\frac{(4+6\alpha)m\pi x}{a_x}\right)\right]\left[\frac{3+6\beta}{4+12\beta}\cos\left(\frac{6\beta n\pi\theta}{\Theta}\right)\right.\right. \\
& \left.\left. - \cos\left(\frac{(2+6\beta)n\pi\theta}{\Theta}\right) + \frac{1+6\beta}{4+12\beta}\cos\left(\frac{(4+6\beta)n\pi\theta}{\Theta}\right)\right]\right\}
\end{aligned}
\tag{3}
$$

Replacing the modal expansion adopted by *w* and the obtained *f* in the nonlinear cylindrical equilibrium equation, Eq. (1), and applying Galerkin's method, obtain a set of second-order nonlinear differential equations in terms of modal amplitudes.

3. NUMERICAL RESULTS

In the present work, considers a cylindrical panel with the following geometrical and physical parameters: R=8.333 m, h=0.01 m, a_x =1 m, a_θ=1 m, E =210 GPa, ν = 0.3 and ρ=7850 kg/m³. The lowest natural frequency for this perfect cylindrical panel without elastic base is ω_0=437.92 rad/s, occurring to wave numbers (m, n) = (1, 1). The presence of the centered elastic base increases the natural frequencies due to the increase in the system stiffness. The study considered the structure with Winkler base with K_w = 46.15 MN/m³ and without Pasternak base K_P = 0, and the presence of initial geometrical imperfection in the shape of the fundamental vibration mode with amplitude equal to $0.05h$. The analysis also investigates three different contact area: a contact area of 1% (ε_1=0.45, ε_2=0.55, ε_3=0.054 and ε_4=0.066), 4% (ε_1=0.4, ε_2=0.6, ε_3=0.048 and ε_4=0.072) and 9% (ε_1=0.35, ε_2=0.65, ε_3=0.042 and ε_4=0.078). The results for the lowest natural frequency of these cylindrical panels are shown in Table 1. A reduced order 2-DOF model ($C_{1,11}(t)$ and $C_{2,22}(t)$) is considered for the transverse displacement field in Eq. (3) because it is able to capture the softening static and dynamic behavior of the cylindrical panel, as presented by Morais e Silva (2019, 2022). From this table, it is worth to note that the presence of a positive initial geometrical imperfection reduces the natural frequency. On the other hand, the presence of the elastic base increases the natural frequency. For the same panel's area, this increasing is less in the unilateral contact base than in the bilateral contact base.

Table 1. Natural frequencies in (rad/s) and non-dimensional frequency (ω/ω_0) for imperfect cylindrical panels, with elastic base of K_w = 46.15 MN/m³ and different contact areas.

Elastic base	**ω(rad/s)**	**ω/ω₀**
Without elastic base	437.18	0.998
Unilateral elastic base on 1% of panel's area	449.28	1.026
Unilateral elastic base on 4% of panel's area	477.23	1.089
Unilateral elastic base on 9% of panel's area	506.62	1.157
Bilateral elastic base on 4% of panel's area	515.39	1.177

Figure 2 displays the frequency-amplitude relation, obtained by the MatCont (Govaerts, 2019), a Matlab software continuation package, for imperfect cylindrical panels, without elastic base (dark blue color), with an elastic base of Winkler K_w = 46.15 MN/m³ and unilateral contact: in 1% of the panel's area (green), 4% of panel's area (black), 9% of panel's area (dark blue) and also by bilateral contact in 4% of panel's area (purple). Figure 2 shows the influence of the elastic base and its area of application on the responses for frequency-amplitude relationship, showing a shifting of the frequency-amplitude relationship curves to the right of the curve of the panel without elastic base (dark blue). It can also be seen in Figure 2 that the non-linear behavior of the frequency-amplitude relationship changes the non-linear softening behavior to an almost linear behavior when the bilateral contact base is considered instead of unilateral contact base.

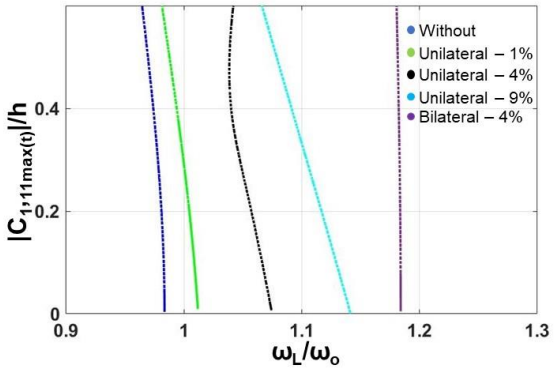

Figure 2. Influence of the elastic base and its area of application on the frequency-amplitude relationship for the cylindrical panels: without elastic base (dark blue color), unilateral elastic base: in 1% of the panel's area (green), in 4% of the panel's area (black), in 9% of the panel's area (dark blue) and bilateral elastic base in 4% of the panel's area (purple).

Now, a time-dependent transversal harmonic distributed load with magnitude P_L = 2.5 kN/m² and excitation frequency ω_L, viscous damping η_1 = 0.01, are applied in the imperfect cylindrical panels with centered elastic base, for different panel's area, and without elastic base. Figure 3 presents the resonance curves of this cylindrical panels, obtained with MatCont, following the same colors used in the analysis of the frequency-amplitude relationship of Figure 2. The Figures 3a and 3b demonstrate the maximum vibration amplitude of the modes $|C_{1,11}max(t)|/h$ and $|C_{2,22}max(t)|/h$ varying with the frequency ratio ω_L/ω_0, respectively.

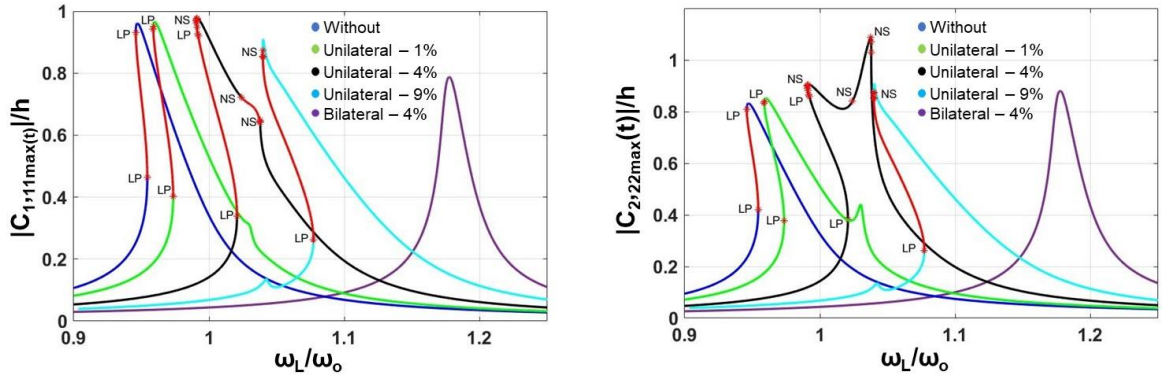

(a) (b)

Figure 3. Resonance curves for different elastic base contact area. (a) $|C_{1,11max}(t)|/h$ and ω_L/ω_0 and (b) $|C_{2,11max}(t)|/h$.

The influence of the elastic foundation on the imperfect cylindrical panel, simply supported, is observed in the resonance curves illustrated in Figure 3. The cylindrical panels without elastic base and with unilateral elastic base contact present similar behavior, when increasing the value of the excitation frequency a vibration amplitude also increases, until it finds an LP bifurcation point (Cycle Limit Point). Then, the resonance curves follow an unstable region (red color), with lower excitation frequency values and higher vibration amplitude, until they find other bifurcation points: LP or Neimark-Sacker bifurcation (NS). After reaching the peak of resonance, the amplitude of vibration shows a smooth decay with increasing excitation frequency. The cylindrical panel with elastic base with unilateral contact in 4% of its area presents a singularity after the resonance peak, an unstable region is found, demarcated by two NS bifurcation points. The cylindrical panel with bilateral elastic base, in 4% of its area, presents an almost linear behavior without bifurcation points. Comparison between the resonance curves for the five cylindrical panels shows how the resonance peaks are shifted to

the right as the contact area with the elastic base increases due to increasing of the natural frequency. The diagrams for the modes |C1,11max(t)|/h and |C2,11max(t)|/h have similar behavior, Figures 3a and 3b. However, the |C1,11max(t)|/h mode has greater amplitudes, because it influences more the nonlinear dynamic behavior of the cylindrical panel. Analyzes of the dynamic behavior and instability of cylindrical panels with unilateral elastic base were studied through phase plane and Poincaré sections by the fourth-order Runge-Kutta method, are illustrated in Figure 4.

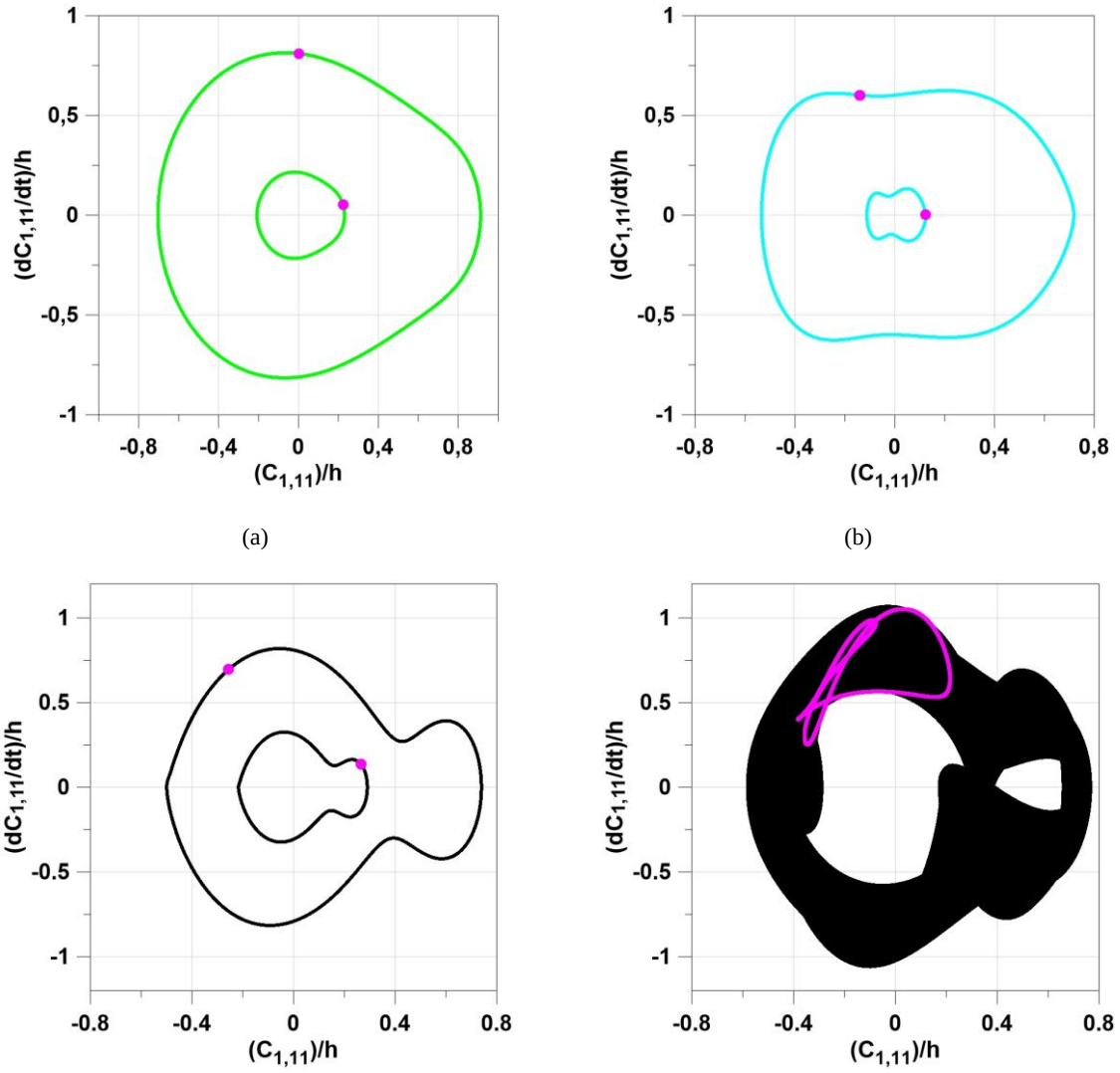

Figure 4. Phase-plane and Poincaré section for: (a) unilateral contact in 1% of panel's area, $\omega_L/\omega_0 = 0.9657$; (b) unilateral contact in 9% of panel's area, $\omega_L/\omega_0 = 1.0600$; (c) unilateral contact in 4% of panel's area $\omega_L/\omega_0 = 1.02$; (d) unilateral contact in 4% of panel's area $\omega_L/\omega_0 = 1.0272$.

Figures 4a shows the phase plane and Poincaré section of the cylindrical panel with unilateral contact in 1% of the area for the ratio $\omega_L/\omega_0 = 0.9657$, for this frequency ratio there are two stable periodic orbits with a period 1T. The cylindrical panel with unilateral contact in 9% of the area also presents phase plane and Poincaré section with a stable periodic orbits with period 1T for the ratio $\omega_L/\omega_0 = 1.0600$, as shown in Figure 4b. Figures 4c and 4d illustrate the phase plane and Poincaré section for the cylindrical panel with unilateral contact in 4% of the area for the ratios $\omega_L/\omega_0 = 1.0200$ and $\omega_L/\omega_0 = 1.0272$, respectively. These phase planes present different behavior. There are a stable periodic orbit with a period 1T for the frequency ratio $\omega_L/\omega_0 = 1.02$ (Figure 4c). However, for the frequency ratio $\omega_L/\omega_0 = 1.0272$, Figure 4d, the Poincaré map describes a closed orbit, that it is a characteristic of a quasi-periodic response, representing a Neimark-Sacker region.

4. CONCLUSION

The influence a non-continuous, unilateral elastic base and an initial geometric imperfection on the nonlinear oscillations and stability of cylindrical panels was studied in this work. The study presents analysis for frequency-amplitude relationship, resonance curves, phase portraits, and Poincaré section for different areas of application of the elastic base. The analyzes consider a modal solution with two degrees of freedom, a consistent model to describe the nonlinear softening behavior of the cylindrical panel. The numerical results demonstrate the impact of the unilateral elastic base applied in different areas of the cylindrical panel, the natural frequency increases with the increase in the area of application of the elastic base, making the system more rigid. However, this increase in natural frequency is less in one-sided contact than in two-sided contact. The frequency-amplitude curves present a shiftning to the right of the panel without an elastic base and change their behavior from non-linear to almost linear as the elastic base changes from unilateral to bilateral hypothesis. The study also shows the influence of the unilateral elastic base on its dynamic stability. The increase in the application area of the unilateral elastic base may present resonance curves with greater instabilities, Neimark-Sacker bifurcation points and Poincaré map with an almost periodic closed orbit. Thus, this work shows the differences that the behavior of cylindrical panels can present for the discontinuous and unilateral elastic foundation, with the presence of geometric imperfections.

5. REFERENCES

Alijani, F., Amabili, M., 2014. Non-linear vibrations of shells: A literature review from 2003 to 2013. Int. J. Non Linear Mech. 58:233-257.

Amabili, Marco; Dalpiaz, Giorgio, 1997. Free vibrations of cylindrical shells with nonaxisymmetric mass distribution on elastic bed. Meccanica, v. 32, p. 71-84.

Amabili, M., Païdoussis, M. P., 2003. Review of studies on geometrically nonlinear vibrations and dynamics of circular cylindrical shells and panels, with and without fluid-structure interaction. Appl. Mech. Rev. 56:349-356.

Babaei, H., Eslami, M. R., 2021. On nonlinear vibration and snap-through buckling of long FG porous cylindrical panels using nonlocal strain gradient theory. Composite Structures, v. 256, n. October 2020, p. 113125.

Bahadori, R., Najafizadeh, M., 2015. Free vibration analysis of two-dimensional functionally graded axisymmetric cylindrical shell on Winkler-Pasternak elastic foundation by First-order Shear Deformation Theory and using Navier-differential quadrature solution methods. Applied Mathematical Modelling, v. 39, n. 16, p. 4877–4894.

Bhattiprolu, U., Bajaj, A. K., Davies, P., 2016. Periodic response predictions of beams on nonlinear and viscoelastic unilateral foundations using incremental harmonic balance method. International Journal of Solids and Structures, v. 99, p. 28–39.

Govaerts, W. et al., 2019. MATCONT: Continuation toolbox for ODEs in Matlab. Retrieved December, v. 4, p. 2020.

Kim, Young-Wann, 2015. Effect of partial elastic foundation on free vibration of fluid-filled functionally graded cylindrical shells. Acta Mechanica Sinica, v. 31, p. 920-930.

Lamprea-Pineda, Angie, C., Connolly, David P., Hussein, Mohammed FM, 2022. Beams on elastic foundations–A review of railway applications and solutions. Transportation Geotechnics, v. 33, p. 100696.

Martins, J. P. et al., 2018. Behaviour of thin-walled curved steel plates under generalised in-plane stresses: a review. Journal of Constructional Steel Research, v. 140, p. 191-207.

Malekjafarian, Abdollah et al., 2021. Foundation damping for monopile supported offshore wind turbines: A review. Marine Structures, v. 77, p. 102937.

Morais, J. L., Silva, F. M. A., 2019. Influence of modal coupling and geometrical imperfections on the nonlinear buckling of cylindrical panels under static axial load. Engineering Structures, v. 183, p. 816-829.

Morais, J. L., Silva, F. M. A., 2022. Nonlinear resonance curves of a cylindrical panel with unilateral contact of a discontinuous elastic base. Proceedings of the XLIII Ibero-LatinAmerican Congress on Computational Methods in Engineering, v. 1. p. 1-7.

Silveira, R. A. M., Pereira, W. L. A., Gonçalves, P. B., 2008. Nonlinear analysis of structural elements under unilateral contact constraints by a Ritz type approach. International Journal of Solids and Structures, v. 45, n. 9, p. 2629–2650.

Song, X., Ren, Y., Han, Q., 2022. Nonlinear vibration of rotating cylindrical shell due to unilateral contact induced tip rubbing impact: Theoretical and experimental verification. Mechanical Systems and Signal Processing, v. 164, n. February 2021, p. 108244.

TJ, H. G. et al., 2006. Free vibration characteristics of cylindrical shells partially buried in elastic foundations. Journal of Sound and Vibration, v. 290, n. 3–5, p. 785–793.

Weitsman, Yechiel, 1971. Onset of separation between a beam and a tensionless elastic foundation under a moving load. International Journal of Mechanical Sciences, v. 13, n. 8, p. 707-711.

Yang, J.; Dong, J., Kitipornchai, S., 2019. Unilateral and bilateral buckling of functionally graded corrugated thin plates reinforced with graphene nanoplatelets. Composite Structures, v. 209, n. September 2018, p. 789–801.

Younesian, D. et al., 2019. Elastic and viscoelastic foundations: a review on linear and nonlinear vibration modeling and applications. Nonlinear Dynamics, v. 97, n. 1, p. 853–895.

Zhao, X. et al., 2022. Review, classification, and extension of classical soil-structure interaction models based on different superstructures and soils. Thin-Walled Structures, v. 173, p. 108936.

6. RESPONSIBILITY NOTICE

The authors are the only responsible for the printed material included in this paper.